Mediterranean Marine Science

Vol 22, No 2 (2021)

VOL 22, No 2 (2021)

Trace-metal distribution and ecological risk assessment in sediments of a sheltered coastal area (Gulf of Gaeta, central-eastern Tyrrhenian Sea, Italy) in relation to hydrodynamic conditions

SIMONE BONAMANO, DANIELE PIAZZOLLA, SERGIO SCANU, VIVIANA PIERMATTEI, MARCO MARCELLI

doi: 10.12681/mms.24996

Mediterranean Marine Science
Indexed in WoS (Web of Science, ISI Thomson) and SCOPUS
The journal is available on line at http://www.medit-mar-sc.net
DOI: http://dx.doi.org/10.12681/mms.24996

Trace-metal distribution and ecological risk assessment in sediments of a sheltered coastal area (Gulf of Gaeta, central-eastern Tyrrhenian Sea, Italy) in relation to hydrodynamic conditions

Simone BONAMANO, Daniele PIAZZOLLA, Sergio SCANU, Viviana PIERMATTEI, and Marco MARCELLI

Ocean Predictions and Applications Division, Centro Euro-Mediterraneo sui Cambiamenti Climatici, Italy
Laboratory of Experimental Oceanology and Marine Ecology, DEB, Tuscia University, Molo Vespucci, Port of Civitavecchia, 00053 Civitavecchia (RM), Italy

Corresponding author: daniele.piazzolla@cmcc.it

Contributing Editor: Helen KABERI

Received: 8 October 2020; Accepted: 17 March 2021; Published online: 17 May 2021

Abstract

This study investigates the relationship between sediment contamination and hydrodynamic conditions in the Gaeta Gulf (Tyrrhenian Sea, Italy), an anthropogenically impacted and sheltered coastal area. The pollution levels, potential toxicity, and ecological risk of trace metals were analysed in 16 sediment sampling sites using Sediment Quality Guidelines (SQGs), the Adverse Effect Index (AEI), and the Mean ERM Quotient (m-ERM-Q). The bottom shear stress of the study area, evaluated using an annual simulation of a 3D numerical model, was used to calculate a new Sediment Mobilisation Index (SMI) that detects the coastal zones where a low probability of sediment resuspension occurs. As, Ni, and Cu concentrations exceeded the Threshold Effects Level (TEL) guideline value and AEI limit in several sampling sites, indicating their ability to produce adverse effects on biota. Moreover m-ERM-Q showed the highest values of potential ecological risk in most of the sampling sites located in the inner part of the Gulf of Gaeta. In this area, the highest SMI values were also identified, demonstrating that there is a tight relationship between the two indexes ($R^2 = 0.8214$). The application of SMI in sheltered areas will help achieve high performance of monitoring and hazard assessment tools through obtaining predictable responses on hotspot identification.

Keywords: Trace metals; sediments; pollution; ecological risk; contamination indices; numerical model.

Introduction

A sheltered or embayed coastal area is generally defined by the presence of one or two natural or artificial impermeable boundaries that cast a degree of curvature on the beach platform (Harley *et al.*, 2005). Sheltered coastal areas occupy 9% of the Italian coast. Of these, 605.5 km are natural stretches, and 104.4 km are artificial stretches (Ferretti *et al.*, 2003). The embayed coastal areas are usually characterised by low wave energies and by abundant sediment accumulation over the long term.

It has been widely reported in the international literature that potentially chemical pollutants, such as trace metals, tend to bind to the finer-particle grain sizes due to its larger surface area and geo-chemical composition (Reddy *et al.*, 2004; Zhang *et al.,* 2014), and then follow the sediment's fate (Windom *et al.*, 1989; Horowitz, 1991; Ligero *et al.*, 2001; Mil-Homens *et al.*, 2013). As a result, the final receptors of pollutants in the sea are the depositional areas of the pelitic fraction which are internationally considered as the main archive of pollutants reflecting the pollution levels in the water column (Chengxin *et al.*, 2002; Selvaraj *et al.*, 2004).

Trace metals are a threat in the marine environment due to their abundance, persistence, and potential toxic effects on marine organisms related to bioaccumulation and biomagnification processes (Liu *et al.*, 2009; Zhan *et al.*, 2010; Ghrefat *et al.*, 2011; Gao & Chen, 2012). Among marine organisms, the benthic community is most exposed to the contaminants present in sediments (Rainbow, 2007; Simpson & Batley, 2007) and can be greatly impacted by them.

However, variations in physical and chemical parameters (e.g., pH, Eh, temperature, and salinity) may cause chemicals to be released from the more stable pelitic deposits. This could lead to adverse effects on many other marine organisms and might affect the ecological quality of ecosystems.

Trace metals levels in sediments are used as a marker to estimate the environmental status and pollution levels in aquatic ecosystems (Caccia *et al.*, 2003). These chemical elements in marine environments can be derived from natural and anthropogenic sources (Zhang *et al.*, 2019). Industrialisation and urbanisation strongly contribute to trace-metal pollution in air, water, soil, and sediments (Nriagu & Pacyna, 1988; Varol, 2011; Chaudhari *et al.*, 2012; Suresh *et al.*, 2011; Bastami *et al.*, 2014). Trace metals released from natural and anthropogenic sources are transported to the marine environment by various pathways including river basin and urban runoff, atmospheric deposition, and sewage discharges.

The hydrodynamic features of the marine environment (e.g., wind, waves, and tides) influence sediment behaviour and consequently the fate of trace metals (Roussiez *et al.*, 2011). In wave-exposed coasts, sediment dynamic mainly consists of intense resuspension and transport processes. On the contrary, in the open sea and sheltered coastal areas, the presence of weaker currents favours the accumulation of sediments and associated pollutants to the seabed.

Water circulation of lagoons, lakes, and sheltered coastal areas has been frequently analysed using hydrodynamic models (Jouon *et al.,* 2006; Grifoll *et al.*, 2014; Cucco *et al.*, 2015; Bonamano *et al.*, 2017). The model results provide hydrodynamic parameters (e.g., age, flushing time, residence time, transit time, and turnover time) that are useful to relate the dynamic processes with pollutants distribution in the marine environment and consequently with the health status of ecosystems (Jouon *et al.,* 2006).

Among the hydrodynamic parameters used in the literature that define the ecological risk in closed and semi-closed environments, bottom shear stress allows for a proper evaluation of the process of mobilisation of marine sediment (i.e., suspension, deposition, and resuspension), which is the basis of the evaluation of the trace-metal contamination in bottom sediments. This hydrodynamic parameter has already been successfully used by Mali *et al.* (2017) within port basins to demonstrate the correlation between bottom shear stress and sediment hazard assessment indexes. This study evaluates the trace metals pollution in bottom sediments of the sheltered coastal zone of Gulf of Gaeta (central-eastern Tyrrhenian Sea, Italy), strongly affected by urbanisation and by the presence of several industrial activities. The aim of this study is also to develop and apply a new index based on the hydrodynamic parameters and verify the correlation with pollution levels in the coastal sediments to use it as a tool for the identification of the potential sampling sites useful for the monitoring and hazard identification program.

Materials and Methods

Study area

The area of interest is the Gulf of Gaeta, located in the Central-Eastern Tyrrhenian Sea, Italy (Fig. 1). It is a non-tidal environment and represents a rocky embayed area as it is enclosed between two coastal sectors with heterogeneous morphology. The northern sector is characterised by high rocky shorelines mainly composed of carbonates while the southern sector shows arenaceous formations and alluvial deposits (Ferretti *et al.*, 1989).

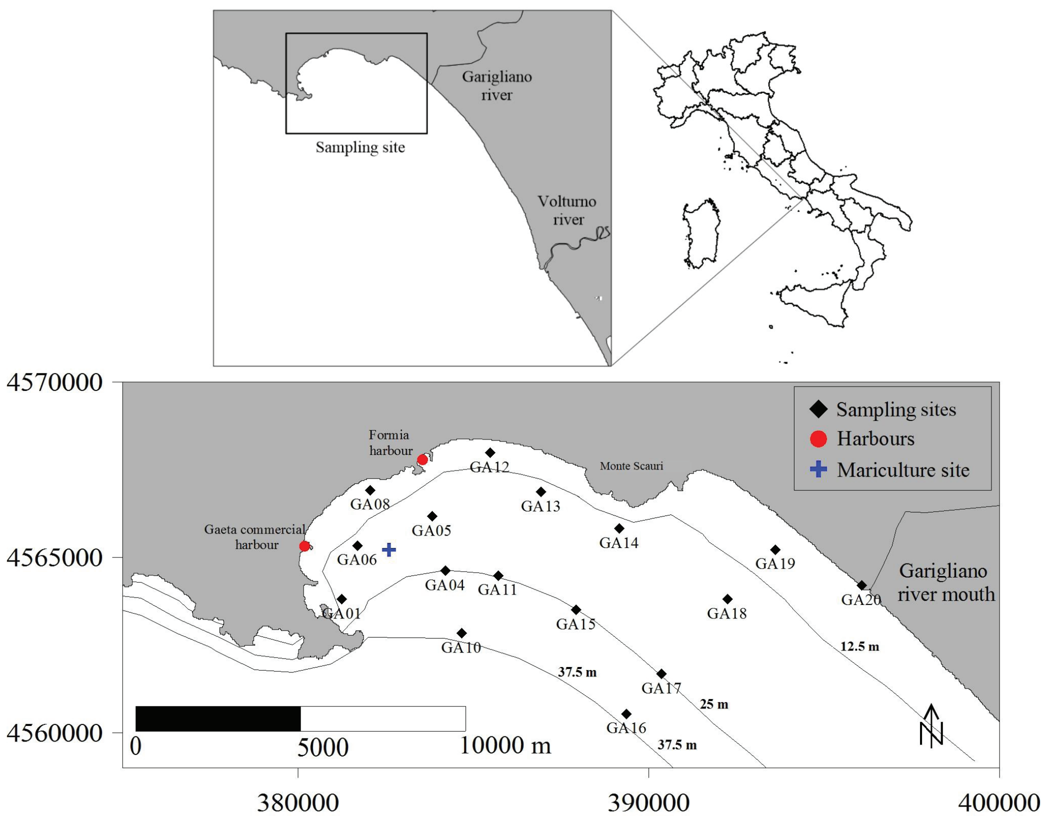

Fig. 1: Study area and sediment sampling sites. The coordinate system is expressed in UTM (WGS84).

This sheltered coastal area (61 km^2) is affected by potential conflicts with the simultaneous presence of both anthropogenic activities (i.e., Gaeta and Formia harbours, mussel and fish farming, tourism facilities) (Orlandi *et al.*, 2014; Paladini de Mendoza *et al.*, 2018) and sensitive zones such as Sites of Community Importance (SCIs; European Union Directive 92/43/EEC) located nearby the gulf.

Four natural watercourses discharge into the Gulf of Gaeta: the Itri and Santa Croce rivers (combined drainage basins of 160.69 km^2), the Minturno river (drainage basin of 3.5 km^2), the Garigliano river (drainage basin of 4984 km^2) (Rossi *et al.,* 2018) and the Volturno river (drainage basin of 5680 km^2), located further to the south of the gulf.

Sediment contributions from Garigliano and Volturno rivers profoundly affect sedimentation in the study area (Ferretti *et al.*, 1989; Maggi *et al.*, 2009). Sediments drained by the Garigliano river are mainly composed of calcite and dolomite, while sediments transported by the Volturno river show abundant quartz, feldspar, and smectite contents (Brondi *et al.*, 1979; Ferretti *et al.*, 1989).

The water circulation of the Central-Eastern Tyrrhenian Sea is composed of a coastal regime, characterised by the formation of secondary cells, and an off-shore regime, dominated by the cyclonic gyre of the Tyrrhenian Sea (De Pippo *et al.*, 2003).

Sediment sampling and analysis

Sediment sampling was performed in July 2018 using a Van Veen grab (18-L volume). Surface sediment samples (n = 16) were collected in 16 sites between 10 and 40 m depth within the Gaeta Gulf and the surrounding area (Fig. 1). The upper (1-4 cm) of sediment of each sample was homogenised, and placed into polyethylene bags. Once transported (at 4° C) to the laboratory, sediments were dried in an oven at 40° C for 48 h and crushed for subsequent analysis.

Grain size analysis was performed through wet sieving on sediments previously treated with dilute (< 10 %) hydrogen peroxide (H_2O_2) to remove organic matter (Spagnoli *et al.* 2014; Shennan *et al.*, 2015). Trace-metal extraction from sediment samples and analytical determination was performed according to the United States Environmental Protection Agency 3050B:1996 and 6010D:2014, respectively. Specifically, 1 g of each sample was weighed and mineralised (DigiPREP system, QuantAnalitica S.r.l - Italy) with a digestion solution prepared using 4.5 mL of hydrochloric acid (HCl) and 1.5 mL of nitric acid (HNO_3) (Carlo Erba Reagents S.r.l – Italy). After digestion, ultrapure water was added to the samples up to 50 mL. Trace metals analysis was performed with an inductively coupled plasma-optical emission spectrometer (ICP-OES; 710 Series, Agilent Technologies S - USA). Standards for the instrument calibration were prepared using a multi-element certified reference solution ICP Standard (Chebios S.r.l – Italy).

To assess the potential toxicity and to verify if a specific metal represents a threat to aquatic ecosystems, concentrations measured in sediment samples were compared with sediment quality guidelines (SQGs), effects range low (ERL), and effects range medium (ERM) determined by Long & Morgan (1990) and later refined by Long *et al.* (1995). The threshold effects level (TEL) and probable effects level (PEL) determined by the Florida Department of Environmental Protection (MacDonald, 1994) were also calculated. Concentrations below TEL or ERL are rarely associated with adverse effects while concentrations above the TEL or ERL, but below PEL or ERM, are occasionally associated with adverse effects; measured concentrations above the PEL or ERM are frequently associated with adverse effects and sediments are predicted to be toxic (Cardellicchio *et al.*, 2007). Subsequently, the adverse effect index (AEI) described by Muñoz-Barbosa *et al.* (2012) was used. AEI is defined using the following equation:

$$AEI = \frac{X}{ERL},$$

where X is the metal concentration, and ERL is the effects range low (Long *et al.*, 1995). If AEI is less than or equal to 1 the trace-metal concentration in the sample is insufficient to produce adverse effects in biota. On the contrary, trace-metal concentration in the sample can produce adverse effects when AEI is greater than or equal to 1 (Muñoz-Barbosa *et al.*, 2012).

Since pollutants occur in the environment as mixtures, it is useful to assess the overall potential toxicity and ecological risk considering multiple anthropogenic contaminations. Thus, the mean ERM quotient (m-ERM-Q, Long & MacDonald 1998; Long *et al.*, 2005; Gao & Chen, 2012) was used. The m-ERM-Q was applied using the following equation (Birch, 2018; Zhang *et al.*, 2019):

$$m - ERM - Q = \sum_{i=1}^{n} \frac{C_i}{ERM_i},$$

where C_i is the metal concentration in the sediment sample, ERM_i is the ERM guideline value for the selected metal, and n represents the number of metals considered. Four classes of toxicity probabilities are defined: m-ERM-Q < 0.1 (9% probability of toxicity); 0.1≤ m-ERM-Q < 0.5 (21% probability of toxicity); 0.5 ≤ m-ERM-Q < 1.5 (49% probability of toxicity); 1.5 ≥ m-ERM-Q (76% probability of toxicity), which denote four respective classes of sediment non-toxic, slightly-toxic, medium-toxic, and highly-toxic (Long *et al.*, 1995; Ahmed *et al.*, 2018).

The natural-neighbour gridding method, included in the software Surfer 8 (Golden Software Inc., USA), was used to analyse the spatial distribution of sediment fraction percentages and trace metals values.

The presence of correlations among trace-metal concentrations and the pelitic fraction percentage was tested. Before correlation analysis, the data distribution was tested using the Shapiro–Wilk test. Because the data were not normally distributed, Spearman's Rank correlation was used; p-value < 0.01 was considered statistically significant. In the 25% of the sampling sites Cu values were below the limit of detection (LOD, 5.0 mg/kg). Thus, Cu data were excluded from the statistical analysis. Finally, a further Spearman's Rank correlation analysis was performed on trace-metal values previously normalised applying the Dilution Factor (Horowitz, 1991) to account for grain-size differences. The Dilution Factor (DL) is given by:

$$DL = \frac{100}{100 - PSF},$$

where PSF represents the percentage of size fraction greater than the range of interest.

Hydrodynamic analysis

In this study, the hydrodynamic analysis was carried out using the DELFT3D models which allows simulating the current field by online coupling between DELFT3D-FLOW (Lesser *et al.*, 2004), that calculates marine currents induced by wind action, and SWAN (Booij *et al.*, 1999), that reproduces the propagation of the wave motion towards the coast.

The set-up of the hydrodynamic model was described by Paladini de Mendoza *et al.* (2018) where it was specified that the DELFT3D-FLOW and SWAN models used the same computational grid that covers the coastal area for about 60 km. Because small errors could occur near the boundaries, the study area was located far from the model edges. The governing equations were solved in a finite difference curvilinear grid with a resolution ranging from 50 m in the area of the Gulf of Gaeta to about 1 km near the off-shore boundary positioned about 30 km from the coast. In the vertical direction, ten sigma layers of equal thickness were considered to allow a greater resolution in the coastal area. A time step of 60 s was chosen to meet the Courant criterion and to reduce the noise introduced by the initial conditions a spin-up time of 1 day was used. The current field was calculated considering the wind drag coefficient linearly changing with its speed (from 0.00063 with 0 m/s to 0.00723 with 100 m/s), eddy viscosity, and diffusivity equal to 1 m^2/s and vertical viscosity determined by k-e turbulence model. The wind data (velocity and direction) were provided by the weather station located inside the Gulf of Gaeta.

In the SWAN, the spectral action balance equation was solved by including the contribution of the terms of bottom friction, whitecapping, and depth induced breaking. In detail, the bottom friction was parametrised using the JONSWAP formulation with a coefficient of 0.067 m^2/s^3, whitecapping was based on the pulse-based model and the breaking was calculated using the Battjes & Janssen model (1978) with a breaking parameter of 0.73. The model was forced with the JONSWAP wave spectrum built using the off-shore wave parameters (significant height, peak period, and mean direction) detected in the study area. Then, the wave effect was included in the DELFT3D-FLOW model by running the SWAN model every 30 min in the online mode.

Using this set-up, the results of both models were validated with surface currents, wave spectral fields, and wave height measured by X-band radar in the Gaeta Gulf during four storm events. The results showed a close correlation between the measured data and model predictions, mainly for the events coming from the south-east direction (Paladini de Mendoza *et al.*, 2018). Given the good reliability of the model in reproducing the current field in the Gulf of Gaeta when it is forced by wind and wave motion, the other forcing of coastal circulation, such as the effect of the river discharge on density variation of the water column, were neglected. This also allowed for a reduction in the computational effort of the model, allowing it to reproduce a long-period circulation pattern (Mali *et al.*, 2017; Lisi *et al.*, 2009) in the Gulf of Gaeta. Specifically, the entire year 2017 (from 1st January 2017 to 1st January 2018) was chosen because it was the most representative period between 2006 and 2019 in terms of wave height and direction.

SMI calculation

To detect the zones where a low probability of sediment resuspension occurs, a new index based on the hydrodynamic model results was developed. The index, called Sediment Mobilisation Index (SMI), was built using the maximum shear bottom stress (mBSS) calculated in the annual simulation in each point of numerical grid. It was calculated as a ratio between the number of times mBSS is less than a given critical value and the total number of model outputs (n). Given that the trace metals were more bounded to the fine fraction of sediment, in this study we have chosen a critical value of mBSS of 0.05 N/m^2 (Gardner, 1989), representing the threshold below which the fine sediment (< 0.063 mm) is not mobilised from the sea bottom.

$$SMI = \frac{n(mBSS < \tau_{max})}{n}$$

To improve the comparison with the m-ERM-Q, the resulting values for each point of the numerical grid were normalised by scaling between 0 and 1.

Values close to 0 indicate that the fine sediment is easily mobilised by waves and currents; while values close to 1 mean that the fine fraction remains on the bottom for a long time, increasing the potential risk of trace-metal contamination in the affected area.

Finally, a comparative analysis was carried out to verify the presence of correlation between the new SMI and the m-ERM-Q, since m-ERM-Q identifies sediment sites with a high probability of toxicity.

Results

The original data set which includes the sampling depth, sandy and pelitic fraction percentages, ranges of trace metals and aluminium, and sediment quality guidelines (ERL/ERM, PEL/TEL), is given in Table 1.

Trace element average concentrations in surface sediments collected from the Gulf of Gaeta followed the order: Zn > Cr > Cu > Ni > Pb > As > Cd. The highest As concentration has been found at the GA08 site while all the other considered trace metals exhibited the highest values at the GA01 site.

Figure 2 shows the spatial distributions of trace metals in sediments as well as the spatial distribution of Al, and sandy and pelitic fraction percentages. The spatial sediment distribution showed a progressive increase of the pelitic fraction from the Garigliano River mouth to the inner part of the gulf (Fig. 2).

The ERM and PEL guidelines were not exceeded in any of the sampling sites (Table 1). However, As exceeded the ERL and TEL guidelines in most of the sediment samples (fourteen and fifteen, respectively out of sixteen in total); Ni exceeded the ERL guideline in seven sampling sites, and the TEL value in ten sampling sites; Cu exceeded the TEL value in five sampling sites.

The AEI values (Fig. 3) show that the As, Ni, and Cu concentrations in sediments could produce adverse effects in biota (AEI > 1). The As values were greater than 1 at all sampling sites except the GA20 sites; Ni showed AEI > 1 values at ten out of sixteen sites; Cu exceeded the AEI threshold at five sampling sites. The highest Cu and Ni AEI values were found in the GA01 site while the highest As AEI value was found in GA08.

The m-ERM-Q (Fig. 3) highlighted slight toxicity (21% probability) of sediments at the GA01, GA04, GA05, GA06, GA08, GA10, GA11, GA15, GA16, and GA17 sites and no toxicity (9% probability) at the GA12, GA13, GA14, GA18, GA19, and GA20 sites.

The distribution of trace metals measured in the Gulf of Gaeta agreed with the pelitic fraction distribution: the greater the fine component of the sediment, the greater the concentration of trace metals in it. This statement was further confirmed by the Spearman's Rank correlation analysis results between the trace metals values and the pelitic fraction percentage (Table 2); all the considered trace metals were positively correlated with the pelitic fraction percentage (p-value < 0.01). Moreover, trace metals appeared positively correlated with each other (p-value < 0.01) as highlighted by the results of the Spearman's Rank correlation analysis performed on trace-metal values previously normalised applying the Dilution Factor (Horowitz, 1991) (Table 3).

Table 1. Trace metals data set.

Sampling Sites	Depth (m)	Pelitic fraction (%)	Sandy fraction (%)	Al (mg/kg)	As (mg/kg)	Cd (mg/kg)	Ni (mg/kg)	Pb (mg/kg)	Zn (mg/kg)	Cr (mg/kg)	Cu (mg/kg)
GA01	15	94	6.45	33600	16.1	0.5	27.7	27	99.7	38	32
GA04	25	92	7.69	22900	13.7	0.37	19.8	8.4	64.7	26	16.4
GA05	17	95	5.44	29900	12.8	0.44	24.6	16	85	34	25
GA06	14	80	20.48	30400	17.9	0.43	24.2	21.6	86.7	32	26.7
GA08	8	76	24.21	25900	20.4	0.45	20.1	15.9	66.9	26	18.1
GA10	35	89	11.14	27800	12.6	0.45	24.1	12.1	77.4	32	21
GA11	24	76	24.35	22300	11.4	0.37	19.7	10.7	65.2	26	17.3
GA12	9	21	79.26	15500	10.4	0.29	13.4	15	47.1	18	10.4
GA13	14	10	89.53	8790	10.7	0.22	8.7	8.2	31.1	12.1	NA
GA14	14	12	88.01	9420	10.3	0.23	9.1	8.3	31	11.8	NA
GA15	25	73	27.49	25200	13.6	0.41	21.6	10	67.8	29	18.6
GA16	35	93	6.74	24800	13.5	0.39	22	11.1	70.2	29	19.3
GA17	24	72	27.74	22400	15.1	0.21	20.2	22	61.8	26	16.7
GA18	15	1	98.67	57400	8.8	0.21	7	5.5	24.5	9.6	NA
GA19	9	4	95.58	7610	8.1	0.24	8.3	7.2	28.7	10.9	NA
GA20	2	4	96.28	8530	4.7	0.26	9.1	8.9	32.6	11.7	5.8
Range	-	1.33 – 94.56	5.44 – 98.67	7610 - 57400	4.7 – 20.4	0.21 – 0.5	7 – 27.7	5.5 – 27	24.5 – 99.7	9.6 – 38	5.8 – 32
ERL	-	-	-	-	8.2	1.2	20.9	46.7	150	81	34
ERM	-	-	-	-	70	9.6	51.6	218	410	370	270
TEL	-	-	-	-	7.2	0.68	15.9	30.2	124	52.3	18.7
PEL	-	-	-	-	41.6	0.76	42.8	112.2	271	160	108

NA – concentrations below the detection limit (LOD)

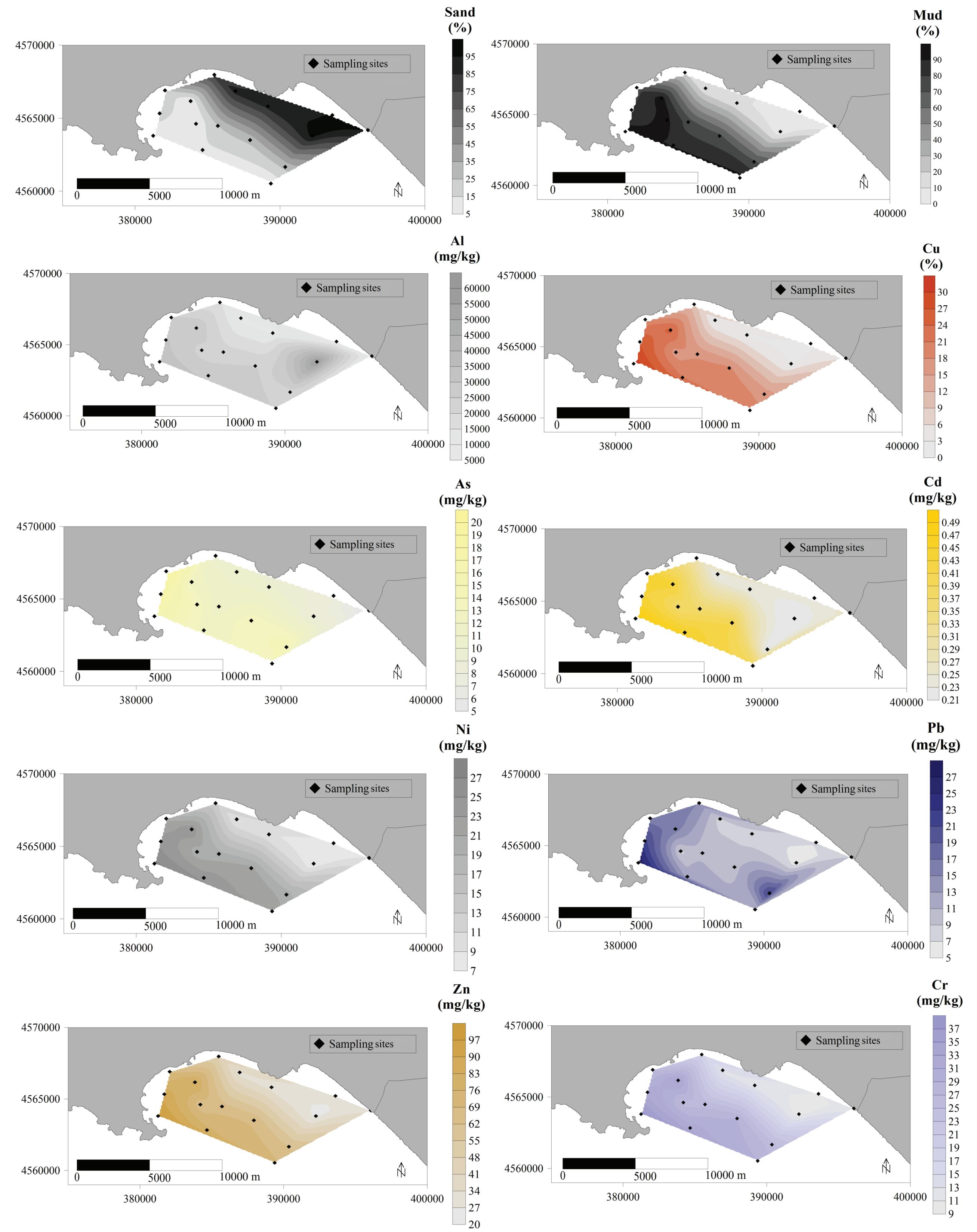

Fig. 2: Spatial distribution of sandy and pelitic fraction percentages, trace metals and Al concentrations. The coordinate system is expressed in UTM (WGS84).

The velocity fields obtained by the DELFT3D-FLOW model were analysed in the three different steps of the annual simulation, corresponding to the meteomarine conditions that favour the resuspension of the fine sediment within the study area. The marine weather conditions examined in this study, ordered in decreasing frequency of occurrence, concern: (i) strong gales and high waves from the West (the West Condition, WC); (ii) intense winds and moderate waves from southern quadrants (the South Condition, SC); and (iii) intense north-eastern gusts of wind coming from Garigliano valley (the Garigliano Condition, GC). Figure 4 shows that higher current

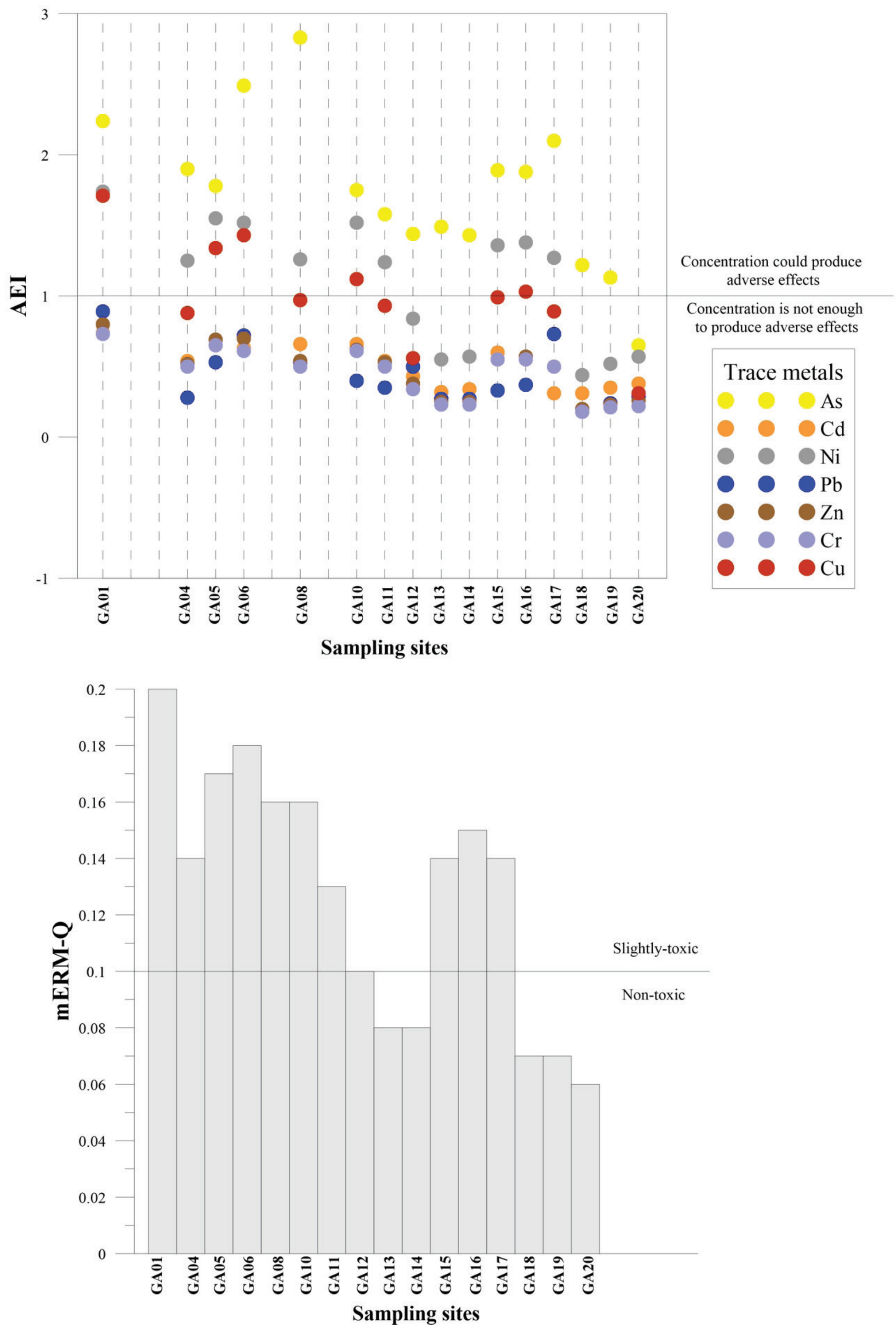

Fig. 3: AEI and m-ERM-Q values at the sampling sites.

Table 2. Spearman's Rank correlation of pelitic fraction and trace metals.

	Pelitic fraction	As	Cd	Ni	Pb	Zn	Cr
Pelitic fraction		1					
As	0.71*	1					
Cd	0.80*	0.60	1				
Ni	0.89*	0.75	0.81	1			
Pb	0.67*	0.73	0.61	0.84	1		
Zn	0.89*	0.74	0.88	0.97	0.79	1	
Cr	0.91*	0.74	0.82	0.98	0.78	0.98	1

* Correlation is significant at 0.01 level

Table 3. Spearman's Rank correlation of normalised trace metals dataset.

	As	Cd	Ni	Pb	Zn	Cr
As	1					
Cd	0.87*	1				
Ni	0.90*	0.90*	1			
Pb	0.89*	0.80*	0.90*	1		
Zn	0.84*	0.94*	0.95*	0.88*	1	
Cr	0.82*	0.87*	0.97*	0.90*	0.96*	1

* Correlation is significant at 0.01 level

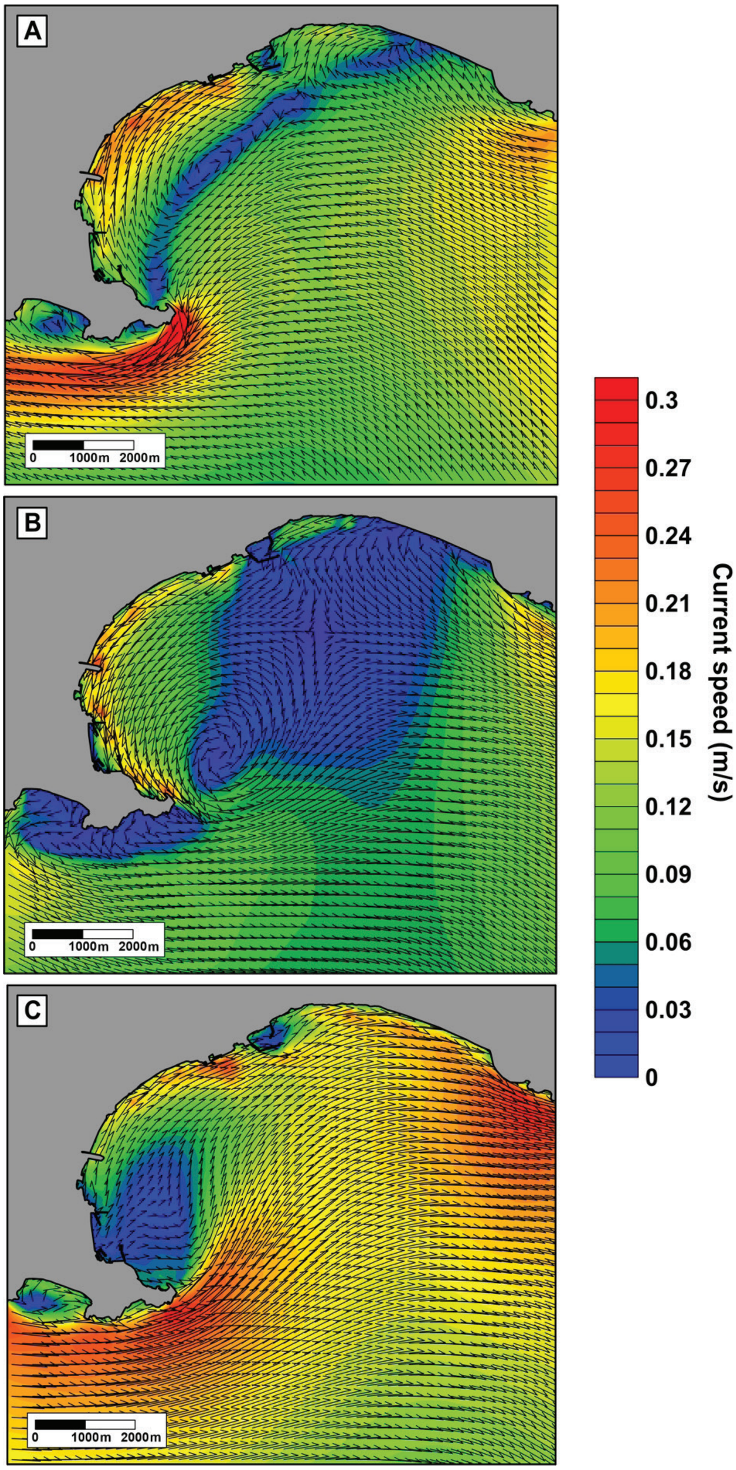

Fig. 4: Velocity fields within the Gulf of Gaeta induced by the South (A), Garigliano (B), and West conditions (C) occurred during the simulation period.

speeds occurred in the proximity of Monte Scauri in the WC and in correspondence to Gaeta promontory in the SC. Within the Gaeta Gulf, high-intensity currents were detected during the Garigliano condition while a large zone with low velocity was found in the WC (Fig. 4).

To evaluate the impact of current speed on the dynamic of fine sediment, the mBSS parameter was computed using the velocity fields calculated by the annual simulation carried out with DELFT3D-FLOW model. The results were then employed to estimate SMI that was used to analyse the movement of the fine fraction through the critical value of 0.05 N/m^2. High index values indicate areas where fine sediments have a high probability of remaining on the bottom, unless rare events coming from the east (e.g., GC) can cause its resuspension, increasing the ecological risk due to trace-metal contamination in the area. Figure 5 shows that the zones with low sediment mobility were located in the south west of the Gaeta Gulf and at a depth greater than 50 m, while a low SMI occurred in the north and in the south coastal zones of the study area (Fig. 5).

SMI was then correlated to the m-ERM-Q as both the indexes describe the potential risk due to high pollutants levels in the bottom sediment. There was a positive linear correlation between the two indices ($R^2 = 0.8214$; r = 0.9063; *p-value* < 0.01) (Fig. 6).

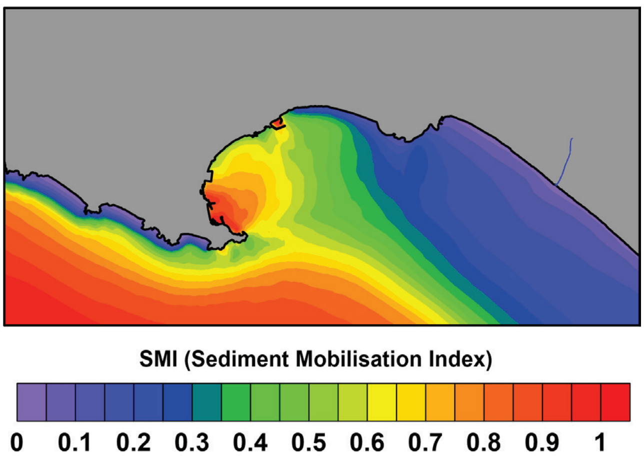

Fig. 5: Sediment Mobilisation index (SMI) distribution in the study area.

Discussion

Several authors have investigated the degree of trace-metal pollution in the bottom sediments of other embayed coastal zones located in the nearby areas (Romano *et al.,* 2009; Mangoni *et al.*, 2016; Trifuoggi *et al.*, 2017) and in the Mediterranean Sea (Acquavita *et al.*, 2010; Di Leonardo *et al.*, 2014; Schintu *et al.*, 2015) (Table 4). Considering the use of different extraction methods, the values of trace metals reported from the literature were comparable to the concentrations measured in this study. However, Pb and Zn values measured in the sediments at the Bagnoli site (Romano *et al.,* 2009; Trifuoggi *et al.,* 2017) were up to 10 times higher than those found in the Gulf of Gaeta due to the presence of the disused steel industrial site.

Sediment fractions distributions (Fig. 2) appeared to be linked to the presence of the Garigliano and Volturno rivers, the influence of which extends up to the Gulf of Gaeta, where sediments finer than those normally found at the same depths occurred, as previously reported by Ferretti *et al.* (1989), and Maggi *et al.* (2009).

The comparison of measured concentrations with SQGs showed that average As, Ni, and Cu concentrations were above the TEL guideline value (Table 1). Furthermore, AEI results (Fig. 3) indicated As, Ni, and Cu contamination in sediments and potential ecological risk in most of the sampling sites.

Trace metals values in sediments of the Gulf of Gaeta appeared positively correlated with each other (Table 3) and followed the distribution of the pelitic fraction percentage (Fig. 2, and Table 2), confirming the existing affinity between pollutants and fine grain-size sediments (Horowitz, 1991; Ligero *et al.*, 2001; Mil-Homens *et al.*, 2013; Xu *et al.*, 2019). Although Cu was excluded from the statistical analysis due to the presence of several values below the LOD, its spatial distribution (Fig. 2) showed a pattern consistent with the other metals. Considering these results, it was possible to assume mutual dependence and a common source for the considered trace metals, likely linked to the influence of the Garigliano and Volturno rivers and governed mostly by sedimentary inputs from the hinterland. Furthermore, the inner part of the Gulf of Gaeta – that showed the highest fine grain-

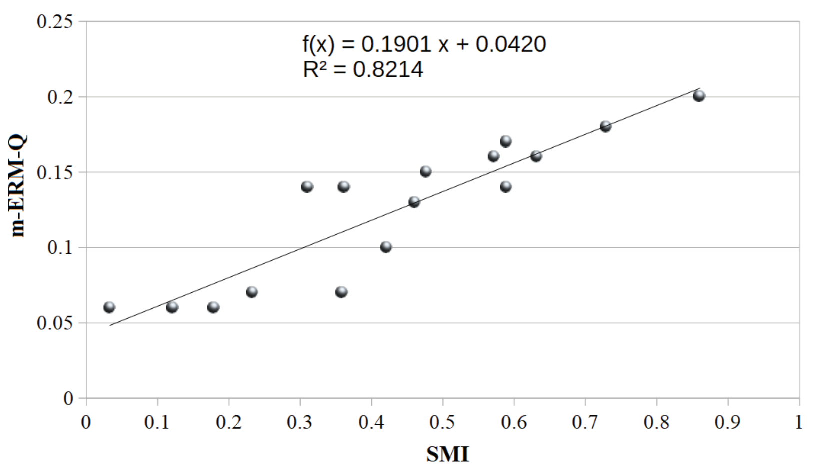

Fig. 6: The relation between SMI and m-ERM-Q evaluated at the 16 sampling sites.

Table 4. As, Cd, Ni, Pb, Zn, Cr, and Cu concentrations (mg/kg) in some Italian coastal areas.

Trace Metals	Range (mg/kg)	Average (mg/kg) ± SD	Location	References
As	4.7 – 20.4	12.51 ± 3.85	Gulf of Gaeta, Tyrrhenian Sea, Italy	*This study*
	-	11	Monte di Procida, Tyrrhenian Sea, Italy	Mangoni *et al.*, 2016
	12.3 – 100.4	35.2	Gulf of Pozzuoli, Tyrrhenian Sea, Italy	Trifuoggi *et al.*, 2017
	0.01 – 19.41	13 ± 10	Bagnoli, Naples, Tyrrhenian Sea, Italy	Romano *et al.*, 2009
	6.4 – 18.2	-	Gulf of Trieste, Adriatic Sea, Italy	Acquavita *et al.*, 2010
	2.39 – 22.9	7.68	Sardinia, Tyrrhenian Sea, Italy	Schintu *et al.*, 2015
	3.1 – 19.7	-	Priolo Bay, Ionian Sea, Italy	Di Leonardo *et al.*, 2014
Cd	0.21 – 0.5	0.34 ± 0.10	Gulf of Gaeta, Tyrrhenian Sea, Italy	*This study*
	-	0.14	Monte di Procida, Tyrrhenian Sea, Italy	Mangoni *et al.*, 2016
	0.0 – 0.7	0.04	Gulf of Pozzuoli, Tyrrhenian Sea, Italy	Trifuoggi *et al.*, 2017
	0.01 – 4.70	0.71 ± 1.16	Bagnoli, Naples, Tyrrhenian Sea, Italy	Romano *et al.*, 2009
	0.16 – 0.45	0.24 ± 0.07	Gulf of Trieste, Adriatic Sea, Italy	Acquavita *et al.*, 2010
	0.02 – 7.34	0.68	Sardinia, Tyrrhenian Sea, Italy	Schintu *et al.*, 2015
	0.1 – 0.2	0.15	Priolo Bay, Ionian Sea, Italy	Di Leonardo *et al.*, 2014
Ni	7 – 27.7	17.48 ± 7.00	Gulf of Gaeta, Tyrrhenian Sea, Italy	*This study*
	-	11	Monte di Procida, Tyrrhenian Sea, Italy	Mangoni *et al.*, 2016
	0.0 – 35.4	9.9	Gulf of Pozzuoli, Tyrrhenian Sea, Italy	Trifuoggi *et al.*, 2017
	3.4 – 181.3	65.5 ± 55.4	Bagnoli, Naples, Tyrrhenian Sea, Italy	Romano *et al.*, 2009
	20 – 231	-	Gulf of Trieste, Adriatic Sea, Italy	Acquavita *et al.*, 2010
	0.5 – 30.3	6.72	Sardinia, Tyrrhenian Sea, Italy	Schintu *et al.*, 2015
	19.6 – 74.9	-	Priolo Bay, Ionian Sea, Italy	Di Leonardo *et al.*, 2014
Pb	5.5 – 27	12.99 ± 6.13	Gulf of Gaeta, Tyrrhenian Sea, Italy	*This study*
	-	21.7	Monte di Procida, Tyrrhenian Sea, Italy	Mangoni *et al.*, 2016
	11.5 – 378.4	105.8	Gulf of Pozzuoli, Tyrrhenian Sea, Italy	Trifuoggi *et al.*, 2017
	21 -1288	260 ± 281	Bagnoli, Naples, Tyrrhenian Sea, Italy	Romano *et al.*, 2009
	12 – 170	-	Gulf of Trieste, Adriatic Sea, Italy	Acquavita *et al.*, 2010
	0.78 – 117.9	4.54	Sardinia, Tyrrhenian Sea, Italy	Schintu *et al.*, 2015
	1.8 – 7.2	-	Priolo Bay, Ionian Sea, Italy	Di Leonardo *et al.*, 2014
Zn	24.5 – 99.7	58.78 ± 23.51	Gulf of Gaeta, Tyrrhenian Sea, Italy	*This study*
	-	54.6	Monte di Procida, Tyrrhenian Sea, Italy	Mangoni *et al.*, 2016
	42.1 – 869.9	224.5	Gulf of Pozzuoli, Tyrrhenian Sea, Italy	Trifuoggi *et al.*, 2017
	111 – 2525	539 ± 538	Bagnoli, Naples, Tyrrhenian Sea, Italy	Romano *et al.*, 2009
	50 – 400	150 ± 85	Gulf of Trieste, Adriatic Sea, Italy	Acquavita *et al.*, 2010

Continued

Table 4 continued

Trace Metals	Range (mg/kg)	Average (mg/kg) ± SD	Location	References
	1.44 – 668.5	95.7	Sardinia, Tyrrhenian Sea, Italy	Schintu *et al.*, 2015
	9.2 – 30.1	19.6	Priolo Bay, Ionian Sea, Italy	Di Leonardo *et al.*, 2014
Cr	9.6 – 38	23.26 ± 9.44	Gulf of Gaeta, Tyrrhenian Sea, Italy	*This study*
	-	10.9	Monte di Procida, Tyrrhenian Sea, Italy	Mangoni *et al.*, 2016
	0.5 – 49.5	14	Gulf of Pozzuoli, Tyrrhenian Sea, Italy	Trifuoggi *et al.*, 2017
	4 – 43	15 ± 8	Bagnoli, Naples, Tyrrhenian Sea, Italy	Romano *et al.*, 2009
	35 – 171	-	Gulf of Trieste, Adriatic Sea, Italy	Acquavita *et al.*, 2010
	2.41 – 64.1	20.03	Sardinia, Tyrrhenian Sea, Italy	Schintu *et al.*, 2015
	5.6 – 20.5	-	Priolo Bay, Ionian Sea, Italy	Di Leonardo *et al.*, 2014
Cu	2.5 – 32	18.94 ± 6.96	Gulf of Gaeta, Tyrrhenian Sea, Italy	*This study*
	-	7.2	Monte di Procida, Tyrrhenian Sea, Italy	Mangoni *et al.*, 2016
	3.5 – 86.2	25.6	Gulf of Pozzuoli, Tyrrhenian Sea, Italy	Trifuoggi *et al.*, 2017
	6 – 165	40 ± 35	Bagnoli, Naples, Tyrrhenian Sea, Italy	Romano *et al.*, 2009
	14 – 70	-	Gulf of Trieste, Adriatic Sea, Italy	Acquavita *et al.*, 2010
	0.5 – 202.6	29.63	Sardinia, Tyrrhenian Sea, Italy	Schintu *et al.*, 2015
	1.5 – 15.7	-	Priolo Bay, Ionian Sea, Italy	Di Leonardo *et al.*, 2014

size component – could be the area mainly subject to the highest potential ecological risk. This hypothesis was in agreement with our results that showed a higher degree of sediment pollution and greater ecological risk in GA01 and GA08 sites (Fig. 3). These two sampling sites were located at low depths and in an area in which m-ERM-Q results identified a slight overall toxicity and ecological risk of sediments (Fig. 3).

The zone with higher trace metal contamination was also characterised by a low current field obtained during the WC, which represents the most frequent condition in the study area, as also highlighted by Paladini de Mendoza *et al.* (2018). High speed values of the sea current in the southern part of the Gulf of Gaeta occur only during the GC which is the least frequent of the meteomarine conditions examined in this study. To demonstrate the dependence between sediment contamination and hydrodynamic conditions, the m-ERM-Q (Fig. 3), which reveals sediment sites with the greatest probability of toxicity, was compared with the new SMI (Fig. 5), based on the hydrodynamic parameters mBSS estimated by the DELFT3D-FLOW model. A close and direct relationship was found between the two indices in the coastal area of Gaeta (Fig. 6), demonstrating that zones with high SMI overlap with those with the greatest probability of sediment toxicity. The fine sediment present in this area is resuspended only during the GC thus becoming a source of contaminants for the water column and biota.

The index developed in this study is sensitive to small variations in environmental stress as it can detect slight toxicity of sediments (according to the m-ERM-Q), such as those detected within the Gulf of Gaeta. SMI can also be easily applied to the potential contamination analysis of other sheltered coastal areas, such as those chosen to compare the results of the trace metals concentration in bottom sediments. It was developed so that it could be modulated on other sediment size classes and used to analyse the potential risk of seabed contamination by other pollutants (e.g., PAH, PCB, chlorinated organic compound, petroleum hydrocarbons, and nutrients). The application of the new index in the embayed areas is relevant for policy and management needs as it will help in the development of high performance monitoring and hazard assessment tools able to confidently identify hotspots (Mali *et al.*, 2017).

Acknowledgements

This research was carried out as a part of the project "*Studio dell'evoluzione morfologica e dei flussi di sedimentazione nell'area del golfo di Gaeta: possibili effetti dei dragaggi portuali" - 2018/2019* (Addendum 4). The authors express their gratitude to the Environmental Office of the Port Authority System of the Central Northern Tyrrhenian Sea for funding the project. Finally, the authors would like to thank Dr. Francesco Paladini de Mendoza and Dr. Riccardo Martellucci for their help in the design and execution of sampling campaigns, respectively. The authors thank the two anonymous reviewers for their valuable comments which helped to improve the manuscript.

References

Ahmed, I., Mostefa, B., Bernard, A., Olivier, R., 2018. Levels and ecological risk assessment of heavy metals in surface sediments of fishing grounds along Algerian coast. *Marine Pollution Bulletin*, 136, 322-333.

Acquavita, A., Predonzani, S., Mattassi, G., Rossin, P., Tamberlich, F. *et al.,* 2010. Heavy metal contents and distribution in coastal sediments of the Gulf of Trieste (Northern Adriatic Sea, Italy). *Water, Air, & Soil Pollution*, 211, 95-111.

Battjes, J.A., Janssen, J.P.F.M., 1978. Energy loss and set-up due to breaking of random waves. In Proceedings of the16th Conference on Coastal Engineering, Hamburg, Germany, 27 August-3 September 1978, pp. 569-587.

Bastami, K.D., Bagheri, H., Kheirabadi, V., Zaferani, G.G., Teymori, M.B. *et al.,* 2014. Distribution and ecological risk assessment of heavy metals in surface sediments along southeast coast of the Caspian Sea. *Marine Pollution Bulletin*, 81, 262-267.

Birch, G.F., 2018. A review of chemical-based sediment quality assessment methodologies for the marine environment. *Marine Pollution Bulletin*, 133, 218-232.

Booij, N., Ris, R.C., Holthuijsen, L.H., 1999. A third-generation wave model for coastal regions, Part I: Model description and validation. *Journal of Geophysical Research*, 104, 7649-7666.

Bonamano, S., Madonia, A., Piazzolla, D., Paladini de Mendoza, F., Piermattei, V. *et al.,* 2017. Development of a predictive tool to support environmentally sustainable management in port basins. *Water*, 9 (11), 898.

Brondi, A., Ferretti, O., Anselmi, B., Falchi, G., 1979. Analisi granulometriche e mineralogiche dei sedimenti fluviali e costieri del territorio italiano. *Bollettino della Società Geologica Italiana*, 98, 293-326.

Caccia, V.G., Millero, F.J., Palanques, A., 2003. The distribution of trace metals in Florida bay sediments. *Marine Pollution Bulletin*, 46, 1420-1433.

Cardellicchio, N., Buccolieri, A., Giandomenico, S., Lopez, L., Pizzulli, F. *et al.,* 2007. Organic pollutants (PAHs, PCBs) in sediments from the Mar Piccolo in Taranto (Ionian Sea, Southern Italy). *Marine Pollution Bulletin*, 55 (10-12), 451-458.

Chaudhari, P.R., Gupta, R., Gajghate, D.G., Wate, S.R., 2012. Heavy metal pollution of ambient air in Nagpur City. *Environmental Monitoring and Assessment*, 184, 2487-2496.

Chengxin, F., Yuxin., Z., Zhijun, J., 2002. Characteristics of the Pollution of Heavy Metals in the Sediments of Yilihe River, Taihu Basin. *Journal of Lake Science*, 14, 235-241.

Cucco, A., Umgiesser, G., 2015. The Trapping Index: How to integrate the Eulerian and the Lagrangian approach for the computation of the transport time scales of semi-enclosed basins. *Marine Pollution Bulletin*, 98, 210-220.

De Pippo, T., Donadio, C., Pennetta, M., 2003. Morphological control on sediment dispersal along the southern Tyrrhenian coastal zones (Italy). *Geologia Romana*, 37, 113-121.

Di Leonardo, R., Mazzola, A., Tramati, C.D., Vaccaro A., Vizzini, S., 2014. Highly contaminated areas as sources of pollution for adjoining ecosystems: The case of Augusta Bay (Central Mediterranean). *Marine Pollution Bulletin*, 89, 417-426.

Ferretti, O., Niccolai, I., Bianchi, C.N., Tucci, S., Morri, C. *et al.,* 1989. An environmental investigation of a marine coastal area: Gulf of Gaeta (Tyrrhenian Sea). p. 171-187. In: Sediment/Water Interactions. Springer, Netherland.

Ferretti, O., Barsanti, M., Delbono, I., Furia, S., 2003. Elementi di gestione costiera-Parte I Tipi morfo-sedimentologici dei litorali italiani.ENEA, Ente per le Nuove tecnologie l‟ Energia el‟ Ambiente.

Gao, X., Chen, C.T.A., 2012. Heavy metal pollution status in surface sediments of the coastal Bohai Bay. *Water Research*, 46, 1901-1911.

Gardner, W.D., 1989. Periodic resuspension in Baltimore Canyon by focusing of internal waves. Journal of Geophysical Research, v. 94, p. 18185-18194.

Ghrefat, H.A., Abu-Rukah, Y., Rosen, M.A., 2011. Application of geoaccumulation index and enrichment factor for assessing metal contamination in the sediments of Kafrain Dam, Jordan. *Environmental Monitoring and Assessment*, 178, 95-109.

Grifoll, M., Jordà, G., Espino, M., 2014. Surface water renewal and mixing mechanisms in a semi-enclosed microtidal domain. The Barcelona harbour case. *Journal of Sea Research*, 90, 54-63.

Harley, M.D., Turner, I.L., Short, A.D., 2015. New insights into embayed beach rotation: the importance of wave exposure and cross-shore processes. *Journal of Geophysical Research: Earth Surface*, 120 (8), 1470-1484.

Horowitz, A.J., 1991. A Primer on Sediment-Trace Element Chemistry, 2nd Edition. Lewis Publishers. Inc., Chelsea MI, 136 p.

Jouon, A., Douillet, P., Ouillon, S., Fraunie, P., 2006. Calculations of hydrodynamic time parameters in a semi-opened coastal zone using a 3D hydrodynamic model. *Continental Shelf Research*, 26 (12), 1395-1415.

Lesser, G.R., Roelvink, J.A., van Kester, J.T.M., Stelling, G.S., 2004. Development and validation of a three-dimensional morphological model. *Coastal Engineering*, 51 (8-9), 883-915.

Ligero, R.A., Ramos-Lerate, I., Barrera, M., Casas-Ruiz, M., 2001. Relationships between sea-bed radionuclide activities and some sedimentological variables. *Journal of Environmental Radioactivity*, 57, 7-19.

Lisi, I., Taramelli, A., Di Risio, M., Cappucci, S., Gabellini, M., 2009. Flushing efficiency of Augusta Harbour (Italy). *Journal of Coastal Research*, 56, 841-845.

Liu, C., Xu, J., Liu, C., Zhang, P., Dai, M., 2009. Heavy Metals in the Surface Sediments in Lanzhou Reach of Yellow River, China. *Bulletin of Environmental Contamination and Toxicology*, 82, 26-30.

Long, E.R., MacDonald, D.D., 1998. Recommended uses of empirically derived, sediment quality guidelines for marine and estuarine ecosystems. *Human and Ecological Risk Assessment*, 4 (5), 1019-1039.

Long, E.R., Morgan, L.G, 1990. The potential for biological effects of sediment-sorbed contaminants tested in the National Status and Trends Program. National Oceanic and Atmospheric Admininistration.

Long, E.R., MacDonald, D.D., Smith, S.L., Calder, F.D., 1995. Incidence of adverse biological effects within ranges of chemical concentrations in marine and estuarine sediments. *Environmental Management*, 19, 81-97.

Long, E.R., Ingersoll, C.G., MacDonald, D.D., 2005. Calculation and uses of mean sediment quality guideline quotients: a critical review. *Environmental Science and Technology*, 40, 1726-1736.

MacDonald, D.D., 1994. Approach to the assessment of sediment quality in Florida coastal waters. Vol. 1. Florida department of environmental protection office of water policy.

Maggi, C., Nonnis, O., Paganelli, D., Tersigni, S., Gabellini, M., 2009. Heavy metal distribution in the relict sand deposits of the Latium continental shelf (Tyrrhenian sea, Italy). *Journal of Coastal Research*, 2, 1237-1241.

Mali, M., De Serio, F., Dell'Anna, M.M., Mastrorilli, P., Damiani, L. *et al.,* 2017. Enhancing the performance of hazard indexes in assessing hot spots of harbour areas by considering hydrodynamic parameters. *Ecological Indicators*, 73, 38-45.

Mangoni, O., Aiello, G., Balbi, S., Barra, D., Bolinesi, F. *et al.,* 2016. A multidisciplinary approach for the characterization of the coastal marine ecosystems of Monte Di Procida (Campania, Italy). *Marine Pollution Bulletin*, 112, 443-451.

Mil-Homens, M., Blum, J., Canário, J., Caetano, M., Costa, A.M. *et al.,* 2013. Tracing anthropogenic Hg and Pb input using stable Hg and Pb isotope ratios in sediments of the central Portuguese Margin. *Chemical Geology*, 336, 62-71.

Muñoz-Barbosa, A., Gutiérrez-Galindo, E.A., Daesslé, L.W., Orozco-Borbón, M.V., Segovia-Zavala, J.A., 2012. Relationship between metal enrichments and a biological adverse effects index in sediments from Todos Santos Bay, northwest coast of Baja California, México. *Marine pollution bulletin*, 64 (2), 405-409.

Nriagu, J.O., Pacyna, J.M., 1988. Quantitative assessment of worldwide contamination of air, water and soils by trace metals. *Nature*, 333, 134-139.

Orlandi, L., Bentivoglio, F., Carlino, P., Calizza, E., Rossi, D. *et al.,* 2014. δ15N variation in *Ulva lactuca* as a proxy for anthropogenic nitrogen inputs in coastal areas of gulf of Gaeta (Mediterranean Sea). *Marine Pollution Bulletin*, 84, 76-82.

Paladini de Mendoza, F., Bonamano, S., Martellucci, R., Melchiorri, C., Consalvi, N. *et al.,* 2018. Circulation during Storms and Dynamics of Suspended Matter in a Sheltered Coastal Area. *Remote Sensing*, 10 (4), 602.

Rainbow, P.S., 2007. Trace metal bioaccumulation: models, metabolic availability and toxicity. *Environment International*, 33, 576-582.

Reddy, M.S., Basha, S., Kumar, V.S., Joshi, H.V., Ramachandraiah, G., 2004. Distribution, enrichment and accumulation of heavy metals in coastal sediments of Alang-Sosiya ship scrapping yard, India. *Marine Pollution Bulletin*, 48 (11-12), 1055-1059.

Romano, E., Bergamin, L., Ausili, A., Pierfranceschi, G., Maggi, C. *et al.,* 2009. The impact of the Bagnoli industrial site (Naples, Italy) on sea-bottom environment. Chemical and textural features of sediments and the related response of benthic foraminifera. *Marine Pollution Bulletin*, 59, 245-256.

Rossi, L., Calizza, E., Careddu, G., Rossi, D., Orlandi, L. *et al.,* 2018. Space-time monitoring of coastal pollution in the Gulf of Gaeta, Italy, using δ15N values of Ulva lactuca, landscape hydromorphology, and Bayesian Kriging modelling. *Marine pollution bulletin,* 126, 479-487.

Roussiez, V., Ludwig, W., Radakovitch, O., Probst, J.L., Monaco, A. *et al.,* 2011. Fate of metals in coastal sediments of a Mediterranean flood-dominated system: an approach based on total and labile fractions. *Estuarine, Coastal and Shelf Science*, 92 (3), 486-495.

Schintu, M., Buosi, C., Galgani, F., Marrucci, A., Marras, B. *et al.,* 2015. Interpretation of coastal sediment quality based on trace metal and PAH analysis, benthic foraminifera, and toxicity tests (Sardinia, Western Mediterranean). *Marine Pollution Bulletin*, 94 (1-2), 72-83.

Selvaraj, K., Mohan, R.V., Piotr, S., 2004. Evaluation of Metal Contamination in Coastal Sediments of the Bay of Bengal, India: Geochemical and Statistical Approaches. *Marine Pollution Bulletin*, 49, 174-185.

Simpson, S.L., Batley, G.E., 2007. Predicting metal toxicity in sediments: a critique of current approaches. *Integrated Environmental Assessment and Management*, 3, 18-31.

Shennan, I., Long, A.J., Horton, B.P. (Eds.), 2015. *Handbook of sea-level research*. John Wiley & Sons.

Spagnoli, F., Dinelli, E., Giordano, P., Marcaccio, M., Zaffagnini, F. *et al.,* 2014. Sedimentological, biogeochemical and mineralogical facies of Northern and Central Western Adriatic Sea. *Journal of Marine System*, 139, 183-203.

Suresh, G., Ramasamy, V., Meenakshisundaram, V., Venkatachalapathy, R., Ponnusamy, V., 2011. Influence of mineralogical and heavy metal composition on natural radionuclide contents in the river sediments. *Appied Radiaion and Isotopes*, 69, 1466-1474.

Trifuoggi, M., Donadio, C., Mangoni, O., Ferrara, L., Bolinesi, F. *et al.,* 2017. Distribution and enrichment of trace metals in surface marine sediments in the Gulf of Pozzuoli and off the coast of the brownfield metallurgical site of Ilva of Bagnoli (Campania, Italy). *Marine Pollution Bulletin*, 124 (1), 502-511.

Varol, M., 2011. Assessment of heavy metal contamination in sediments of the Tigris River (Turkey) using pollution indices and multivariate statistical techniques. *Journal of Hazardous Materials*, 195, 355-364.

Windom, H.L., Smith, R.G. Jr, Rawlinson, C., 1989. Particulate trace metal composition and flux across the south eastern US continental shelf. *Marine Chemistry*, 27, 283-297.

Xu, J., Xu, L., Zheng, L., Liu, B., Liu J. *et al.,* 2019. Distribution, risk assessment, and source analysis of heavy metals in sediment of rivers located in the hilly area of southern China. *Journal of Soils and Sediments*, 1-12.

Zhan, S., Peng, S., Liu, C., Chang, Q., Xu, J., 2010. Spatial and temporal variations of heavy metals in surface sediments in Bohai Bay, North China. *Bulletin of Environmental Contamination and Toxicology*, 84, 482-487.

Zhang, C., Yu, Z.G., Zeng, G.M., Jiang, M., Yang, Z.Z. *et al.,* 2014. Effects of sediment geochemical properties on heavy metal bioavailability. Environment international, 73, 270-281.

Zhang, H., Walker, T.R., Davis, E., Ma, G., 2019. Ecological risk assessment of metals in small craft harbour sediments in Nova Scotia, Canada. *Marine Pollution Bulletin*, *146*, 466-475.